F.F. Lavrentev; O.P. Salita; Pavel Lukáč
Low temperature strain hardening and dislocation structure formation in HCP crystals

Acta Universitatis Carolinae. Mathematica et Physica, Vol. 23 (1982), No. 2, 33--59

Persistent URL: http://dml.cz/dmlcz/142494

Low Temperature Strain Hardening and Dislocation Structure Formation in HCP Crystals

F. F. LAVRENTEV, O. P. SALITA

Physico-Technical Institute of Low Temperatures, Academy of Sciences of the Ukrainian SSR, Kharkov*)

P. LUKÁČ

Department of Metal Physics, Charles University, Prague**)

Received 30 September 1982

The purpose of this paper is (a) to present a critical review of new experimental results obtained on h.c.p. metals in a wide temperature range, (b) to give new information on the dislocation structure, (c) to examine relations between the dislocation structure and the anomalies of the low temperature plasticity, and (d) to indicate possible mechanisms of the low temperature deformation behaviour.

Důvodem k napsání tohoto článku byl (a) kritický přehled nových experimentálních výsledků, získaných na hexagonálních kovech s nejtěsnějším uspořádáním v širokém teplotním oboru, (b) podat nové informace o dislokační struktuře, (c) vyšetřit vztahy mezi dislokační strukturou a anomáliemi plasticity za nízkých teplot a (d) vytypovat možné mechanismy pro nízkoteplotní deformaci.

Целью статьи является а) критический обзор новых результатов полученых при исследовании гексагональных металлов с полной упаковкой в широком температурном промежутке, б) дать новые информации о дислокационной структуре, в) рассматривать отношение дислокационой структуры и низкотемпературных аномалий и г) установить возможные механизмы низкотемпературной деформации.

1. Introduction

Investigations of the temperature influence on the process of plastic deformation of metallic crystals with different structures (f.c.c., b.c.c. and h.c.p.) have shown that the temperature dependences of parameters of the work hardening curve obtained experimentally at very low temperatures differ from those theoretically predicted. So the low temperature dependence of the critical resolved shear stress (C.R.S.S.) [1] shows deviations from the classically expected increase of the CRSS with decreasing temperature [2]. A number of new results obtained in many other experi-

*) Kharkov — 86, Lenin's Prospect 47, USSR.

**) 121 16 Praha 2, Ke Karlovu 5, Czechoslovakia.

ments give more information concerning the rate-controlling mechanisms which effect the observed phenomenon especially: the thermodynamics of the processes of yielding [3]; the effect of solute concentration on the temperature dependence of the yield stress [4–6]; changes in short-range and long-range stresses with temperature [3] etc.

A survey of the work done till 1974 on the low temperature plastic deformation can be found in [1,7–10]. The purpose of this paper is to present new experimental results obtained on h.c.p. metals deformed at low temperatures in order to clarify their relations to the diclocation structure and to indicate possible mechanisms of low temperature anomalies of plastic deformation. No attempt, however, has been made to summarize all of the relevant papers. We would like to apologize to unreported authors.

2. Low temperature plastic deformation

2.1. The temperature dependence of the shear stress – shear strain curves

In recent years much work has been done on the temperature dependence of the shear stress – shear strain curves of metal single crystals deformed in tension [11], compression [12, 13] and simple shear strain [14].

Fig. 1 shows the shear stress – shear strain curves of Cd single crystals deformed in a wide temperature range from 4.2 to 295 K. It is seen that the shear stress – shear

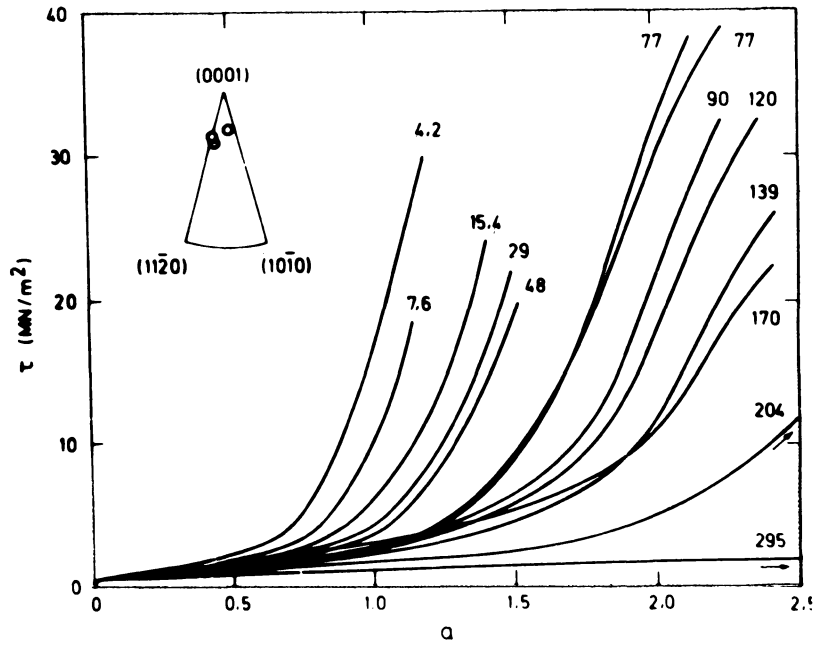

Fig. 1. Work hardening curves for Cd single crystals deformed at temperatures between 4.2 and 295 K [11].

strain curves at all temperatures consist of two stages. At higher temperatures the three stages hardening curve is a rather general phenomenon. It should be noted that for h.c.p. metals the first stage – stage A (sometimes called easy glide range) – is generally much longer than for f.c.c. metals. The extent of the easy glide decreases with decresing temperature. The slope of the easy glide range (work hardening coefficient) ϑ_A is also sensitive to temperature.

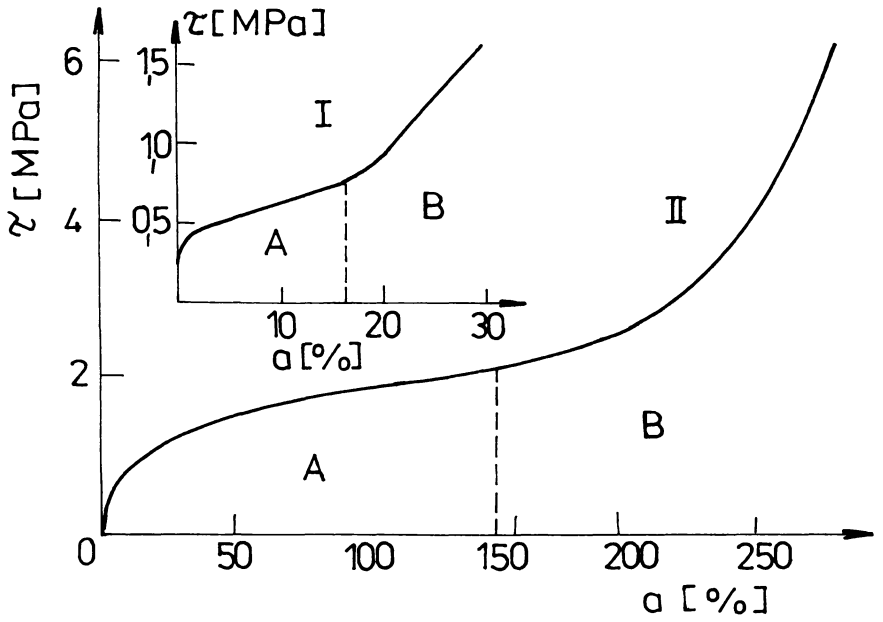

Fig. 2. Work hardening curves for Cd single crystals deformed by compression (curve I) and by simple shear (curve II) [14, 15].

A typical hardening curves for Mg single crystals investigated in compression test [15] and by the simple shear strain technique [14] at 300 K are shown in Fig. 2. Similar curves has been obtained over the temperature range from 4.2 to 300 K, too.

It ought to be noted that the three stages work hardening curve is a general phenomena even if values of the parameters of work hardening curves are dependent on the deformation method. Thus, e.g., the extent of the easy glide region of a crystal deformed by the simple shear strain technique is higher than that of deformed by tension or compression (see Fig. 1 and Fig.2). The value of the work hardening rate ϑ_A for crystals deformed by compression is higher that that for crystals deformed in tension or by simple shear strain technique.

The nature of changes in parameters of the shear stress-shear strain curves with the deformation method will be given in the following parts.

2.2. The effect of temperature on the critical resolved shear stress

The temperature dependence of the critical resolved shear stress τ_o of hexagonal metal crystals deformed in the shear strain condition at very low temperatures has been investigated extensively by Vladimirova [16] and Lavrentev [8]. The critical resolved shear stress for both Cd and Zn [8, 16, 17] at temperatures below 40 K decreases with decreasing temperature. This result is in contradiction to the theory of Seeger [2] and the earlier results of Schmid and Boas [18].

The dislocation structure (dislocation density and dislocation arrangement) can influence the deformation behaviour of single crystals. There is also well known that τ_o is strongly temperature dependent in the presence of solute atoms. The temperature dependence of τ_o for Zn single crystals with various purity is shown in Fig. 3 [4]. It is clearly evident that the critical resolved shear stress does not increase with decreasing temperature in the whole temperature range studied. The function $\tau_o = \tau_o(T)$ is non-monotonous. At temperatures between 300 and 40 K an increase of τ_o with decreasing temperature is observed, which is in agreement with the nature of thermally activated glide. The critical resolved shear stress $\tau_o(T)$ shows a relative maximum at $T = 30-40$ K and a minimum at $T = 10-15$ K. As temperature is decreasing down to 1.5 K the CRSS increases very rapidly. In contrast to the result obtained by Lavrentev [8] who observed a maximum in the temperature dependence of the CRSS at 40 K, Fig. 3 shows new effects. It is obvious from Fig. 3 that the maximum and the minimum in the temperature dependence of the CRSS are not influenced by impurities in zinc single crystals. However, a decrease in impurity content is accompanied by a marked decrease in the CRSS in the whole temperature interval investigated and also by reducing of the maximum and by a lowering of the rate of the CRSS increase with temperature $(d\tau_o/dT)$ in the neighbourhood of the maximum. In the temperature range from 1.5 to 10 K a very rapid increase in the CRSS with decreasing temperature is observed. The values of $d\tau_o/dT$ in this temperature interval are given in Table 1 for zinc single crystals of various impurity contents.

A non-monotonous temperature dependence of the CRSS (like that in Fig. 3) has been also observed for cadmium single crystals alloyed with zinc as in Fig. 4 [6].

Table 1

The maximum values of $d\tau_o/dT$ [kPa/K] for different intervals in the temperature dependence of the CRSS

Purity of zinc	Temperature intervals		
	77—40 [K]	40—10 [K]	10—1.5 [K]
99.98%	−9.10	14	−180
99.997%	−3.25	7	−202
99.9995%	−1.95	4	−231

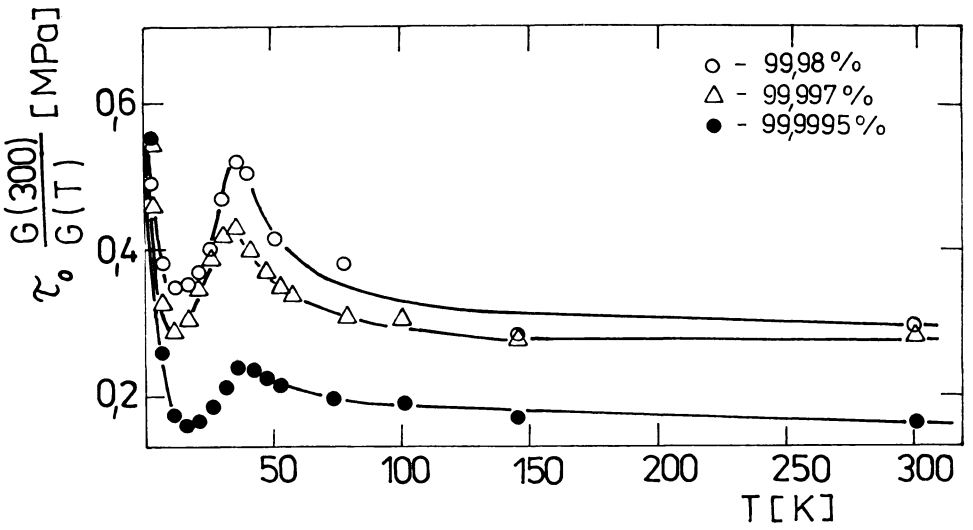

Fig. 3. Temperature dependence of the critical resolved shear stress for zinc single crystals of purity 99.98 (○), 99.997 (△), 99.9995 (●) deformed by simple shear [4].

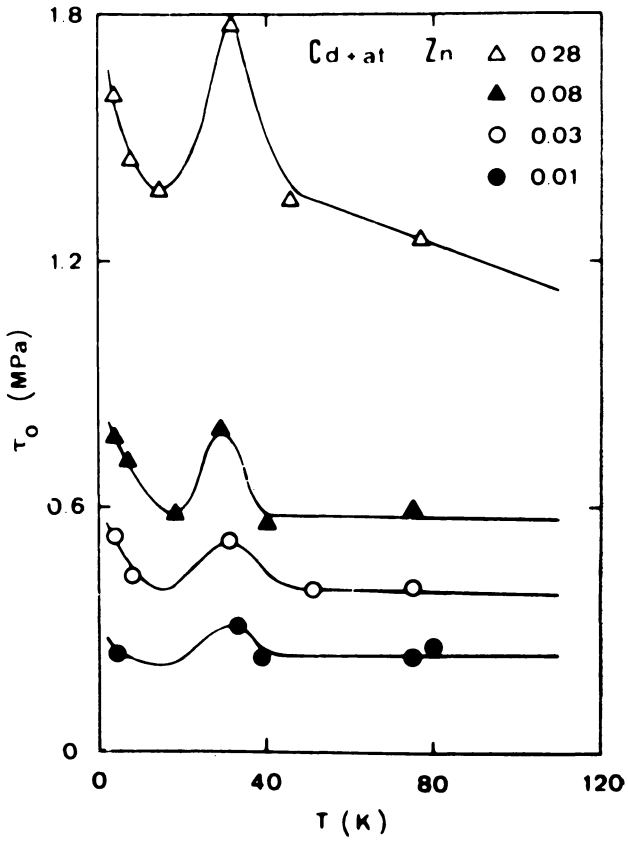

Fig. 4. Temperature dependence of the critical resolved shear stress for cadmium single crystals alloyed with zinc deformed by tension [5].

A maximum in the temperature dependence of the CRSS occurs at 30 K. The CRSS at 30 K is about 30 MPa for Cd + 0.01 at.% Zn single crystals and about 1.8 MPa for Cd + 0.28 at.% Zn. With decreasing temperature between 30 K and 12 K the CRSS decreases and reaches a relative minimum at 12 K whereas the further decrease in temperature from 12 K to 3.2 K causes a distinct increase in the CRSS. A similar temperature dependence of the CRSS has been obtained for cadmium single crystals

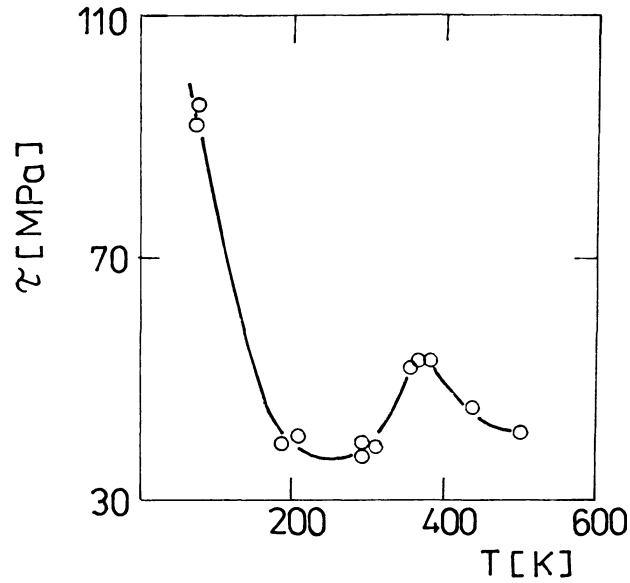

Fig. 5. Temperature dependence of the critical resolved shear stress of magnesium single crystals for $\{11\bar{2}2\}\ \langle 11\bar{2}3\rangle$ pyramidal slip system [22].

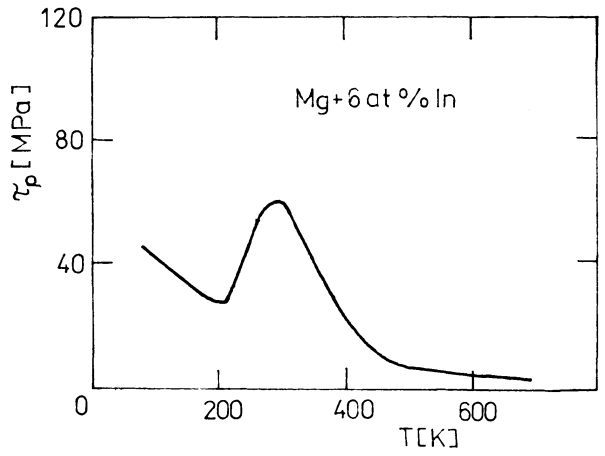

Fig. 6. Temperature dependence of the critical resolved shear stress of magnesium-indium single crystals for $\{1\bar{1}00\}\ \langle 11\bar{2}0\rangle$ prismatic slip system [23].

alloyed with silver, too [5]. One can conclude that Zn as well as Ag atoms (as solute) in Cd have qualitatively the same influence on the temperature dependence of the CRSS as impurities in zinc single crystals. For very pure zinc as well as cadmium single crystals the temperature dependence of the CRSS should be monotonous and very weak. This statement can be supported by the influence of Ni on the temperature dependence of the CRSS of Cu single crystals observed by Suzuki [19].

The peculiarities in the temperature dependence of the CRSS have been observed not only when the values of the CRSS have been obtained by means of active deformation with a constant shear strain rate [3, 4, 6, 16] but also when the deformation experiments were made using a creep technique [5, 20, 21].

It is interesting to note that the nonmonotonous temperature dependence of the CRSS is observed not only for glide in basal plane but also for pyramidal and prismatic slip. Fig. 5 shows an example of the temperature dependence of the CRSS for pyramidal slip system $\{11\bar{2}\bar{2}\}\langle 11\bar{2}3\rangle$ in Mg single crystals [22]. It is seen that the observed temperature dependence of the CRSS with a maximum at 360 K is qualitatively similar to those shown above. The temperature dependence of the CRSS for prismatic slip $\{1\bar{1}00\}\langle 11\bar{2}0\rangle$ in Mg + 6 at.% In is presented in Fig. 6 [23]. A relative maximum of the CRSS at about 300 K is observed, whereas a relative minimum occurs at about 200 K. We believe that this temperature behaviour of the CRSS is influenced by indium solute atoms because the temperature dependence of the CRSS for prismatic slip in pure magnesium is monotonous [24, 25]. The temperature dependence of the CRSS for prismatic slip of Mg single crystals containing Li is very complex [24]. The nonmonotonous temperature dependence of the CRSS for prismatic slip has been observed for Be + 0.23 at.% Cu and Be + 1.34 at.% Cu [26].

2.3. Temperature and strain rate dependence of the work hardening rate (coefficient)

In earlier measurements [18] the work hardening rate ϑ_A in stage A of the work hardening curve of h.c.p. metals were estimated at temperature points which were distant from one another.

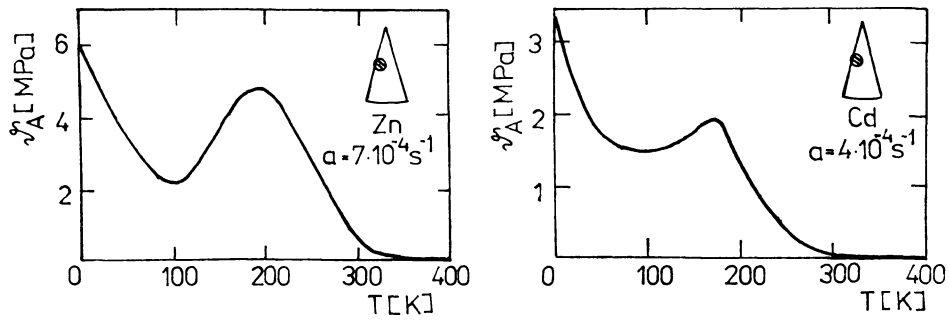

Fig. 7. Temperature dependence of the work hardening rate in stage A for a) zinc single crystals, b) cadmium single crystals [27].

The work hardening behaviour of Cd, Zn and Mg has been investigated in a wide temperature range [11, 15, 27, 28]. From Fig. 7 and Fig. 8 it is seen that the temperature dependence of the work hardening rate for both zinc (at $\dot{a} = 7 \times 10^{-7}\,s^{-1}$) and cadmium (at $\dot{a} = 4 \times 10^{-4}\,s^{-1}$) is very similar, At low temperatures below 100 K for Zn and 60 K for Cd resp. the work hardening rate decreases with increasing

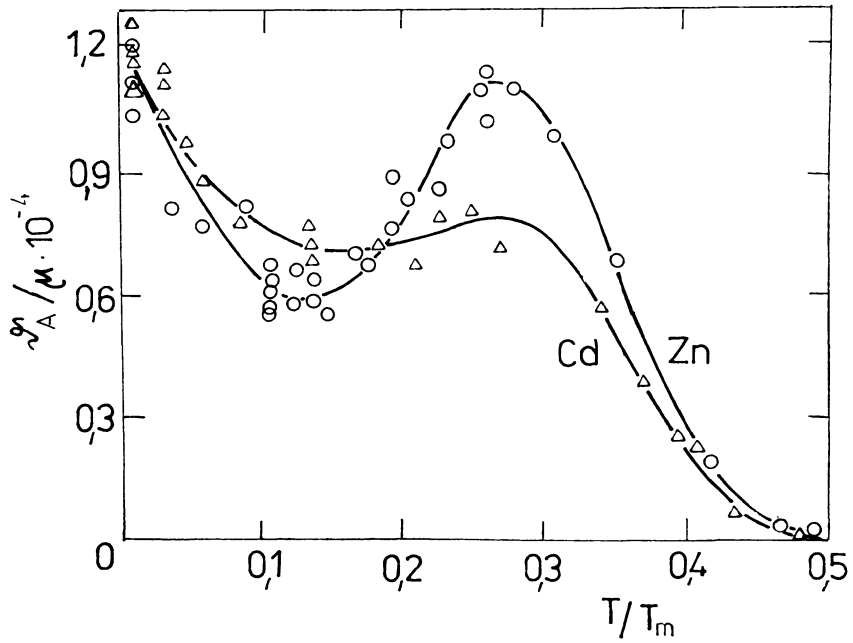

Fig. 8. Reduced work hardening rates of Zn and Cd versus homologous temperature [27].

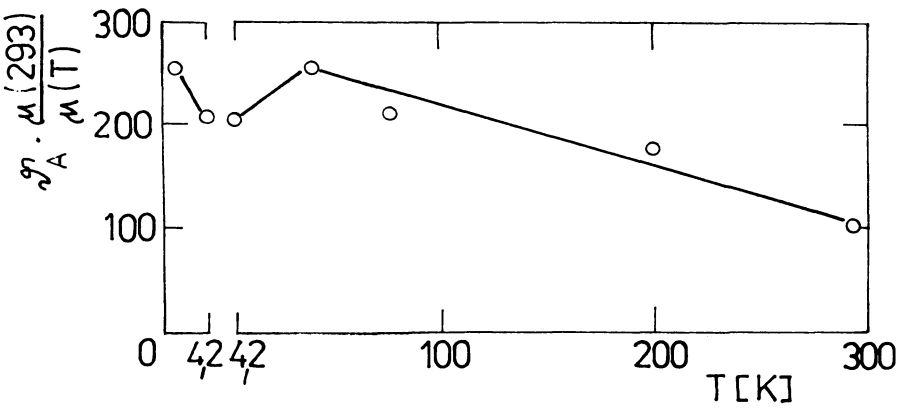

Fig. 9. Temperature dependence of the work hardening rate for magnesium single crystals deformed by simple shear [15].

temperature. The maximum value of ϑ_A at $T/T_m = 0.3$, where T_m is the melting point, depends on the strain rate [27]. The temperature dependence of ϑ_A for Mg single crystals obtained by Lavrentev and Sokolovskiy [15] shown in Fig. 9 is very similar to those for Cd and Zn single crystals given in Fig. 7 and Fig. 8. Note that the Cd and Zn single crystals used were deformed by tension whereas Mg single crystals by simple shear. It has been shown by Pokhil [14] that the type of stressed state (tension, compression, simple shear) can influence the parameters of the work hardening curve for Mg single crystals under basal slip. On the other hand a similar temperature dependence of ϑ_A has been obtained for both Zn and Cd single crystals deformed using a creep technique [20].

It is difficult to explain the above-mentioned temperature dependence of the work hardening rate by existing theories [2, 29], which do not predict the increase of ϑ_A with decreasing temperature at temperatures below $0.3\ T_m$. At temperatures higher than $0.3\ T_m$ the work hardening rate depends on the strain rate [27–30], too.

2.4. Temperature dependence of the stage extension

The temperature dependences of the stage lengths could help to identify deformation processes of hexagonal metals. However there is little information concerning these dependences. The temperature dependence of the length of stage A of the work hardening curve has been studied for both Cd [11] and Mg [15] single crystals in the temperature range 4.2 to 300 K. Fig. 10 shows the temperature dependence of the length of the ease glide stage a_A for Cd and Mg. It is seen that with decreasing temperature the length a_A decreases from $a_A = 2.2$ and $a_A = 2.0$ at 295 K to $a_A = 0.6$ and $a_A = 0.9$ at 4.2 K for Cd and Mg, respectively.

It should be noted that for Mg single crystals the local minimum of ϑ_A at 4.2 K (Fig. 9) corresponds to the local maximum of a_A at 4.2 K (Fig. 10b).

Figure 10a also shows the temperature dependence of a_m, the shear strain at the maximum slope of the work hardening curve for Cd single crystals.

It is necessary to note that the measured temperature dependence of the parameters of the work hardening curve for f.c.c. metals differ distinctly from those for h.c.p. metals. The main differences are the following:

1) the length of easy glide increases with increasing temperature for h.c.p. metals whereas it decreases for f.c.c. metals [2, 31].

2) the work hardening rate decreases with increasing temperature for h.c.p. metals, while it is increasing for f.c.c. metals [2, 31].

3) the maximum value of the reduced work hardening rate (ϑ_{max}/μ, where μ is the shear modulus) decreases rapidly with increasing temperature for h.c.p. metals, while it is not only temperature independent but it also has practically the same value for f.c.c. metals [2, 31].

The likely causes of these differencies will be consider in the following parts of this paper.

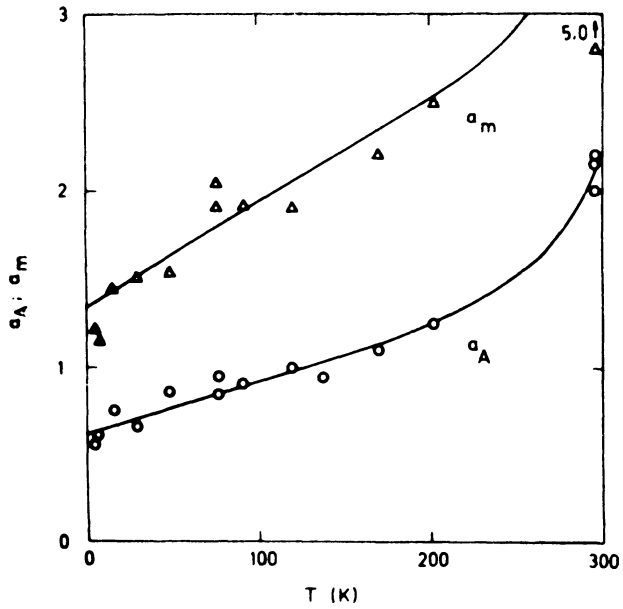

a)

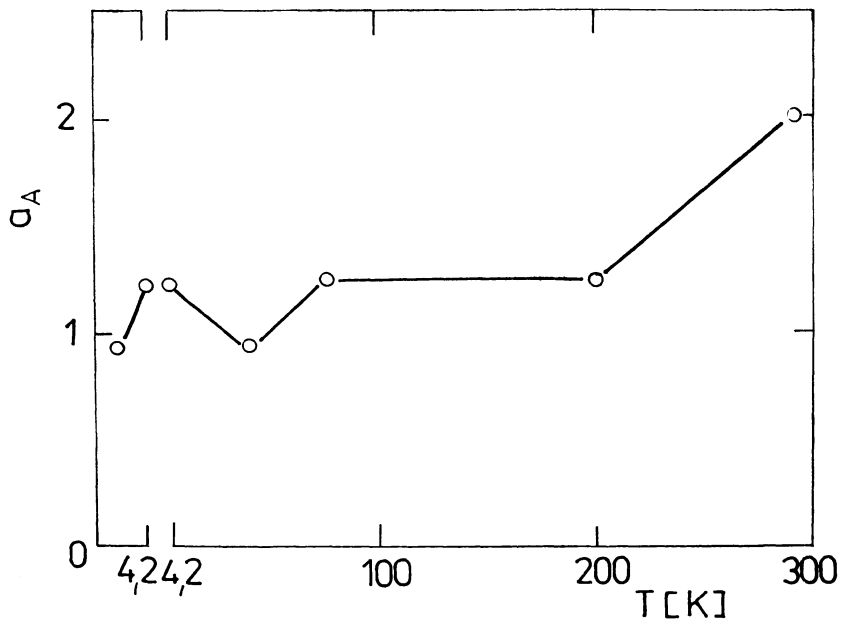

b)

Fig. 10. Temperature dependence of the length of stage *A* a) for cadmium single crystals deformed by tension [11], b) for magnesium single crystals deformed by simple shear [15].

3. Dislocation structure formed during deformation of h.c.p. metals

At the present time, there are few sets of the available experimental data regarding the evolution of dislocation structure in metals under the shear stress at various temperatures. It can be due to experimental difficulties in study, identification and elaboration of the investigated structural changes in materials. On the other hand those investigations are necessary in order to understand strengthening mechanisms, to explain the stability of dislocation structure under termomechanical treatment, to find techniques through which more precise crystalline solids may be prepared and to try to solve other problems of solid state physics.

3.1. Dislocation structure and mechanical properties

At the present time, dislocation structure in magnesium single crystals in a wide temperature range in the course of deformation is probably investigated the most fully [8, 14, 32–35]. These experiments cover the whole work hardening curve. The dislocation structure in Mg single crystals is stable at room temperature and therefore it is suited for the study of the dislocation dynamics and kinetics in the course of plastic deformation.

The dislocation structure in Mg single crystals was investigated very intensively under basal slip at room temperature for the case of tension [32, 34] and simple shear [8, 13, 14, 36]. It has been found that at the beginning of stage A (under both deformation methods) individual dislocations and dipoles of edge types are observed which correspond to the most loaded basal slip system. The dislocation distribution is sufficiently inhomogeneous, there are vast regions containing no defects [8, 14, 37] as shown in Fig. 11. Typical also is the absence of dislocations not only in the crossing slip systems but with the secondary basal Burgers vectors, too. The most typical elements of the dislocation structure in stage A are the edge dipoles formed due to interaction between dislocations in the parallel basal plane with Burgers vector corresponding to the most loaded basal slip system. It has also been found that dipoles and multipoles are formed not only under basal slip but also in the slip in prismatic and pyramidal planes.

The role of dipoles and multipoles in strain hardening can be found e.g. in [32, 34, 38, 39]. From this one may conclude that the strain hardening at the onset of plastic deformation is likely to be controlled by the long-range internal stress field from uniformly distributed dislocations of the same sign.

If the deformation increases (up to about 100%) one can observe the dislocations which belong to the less loaded basal slip systems. The secondary basal dislocations interact with the primary ones. As the result the recombination of dislocations in the same basal plane takes place or dipoles in the case of dislocation in parallel planes are formed. The total dislocation density increases with the shear strain and dislocation distribution becomes more regular. The beginning of the active slip of the secondary

Fig. 11. Dislocation structure of magnesium single crystal at the early stage of deformation [8].

Fig. 12. Dislocation structure of magnesium single crystal at stage A (about 100%) of the work hardening curve [37].

basal dislocations allowing the dislocation reactions between the basal dislocations with different Burgers vectors leads to the situation when at the end of stage A the dislocation network on the basal plane is a characteristic structure element (see Fig. 12).

The transition from stage A to stage B of the work hardening curve is characterized (as in the case of compression deformation [8]) by cross slip of the basal screw dislocations. After the cross slip jogs in the $\{10\bar{1}0\}$ planes can be formed. Ac-

cordingly, a complex cellular structure is produced in the basal planes (Fig. 13). As the deformation is increased prismatic forest dislocations are observed in the cross-section $\{10\bar{1}0\}$ perpendicular to the primary (basal) slip plane. Lavrentev [8] has shown that the forest dislocations formed in magnesium during deformation are tied with the primary dislocations (both dislocations type have the same Burgers vector), because the prismatic slip is generated in the cross-sliping dislocation segment of the screw basal dislocations.

Fig. 13. Dislocation network observed in basal plane at stage *A* (about 100%) of the work hardening curve of magnesium single crystal [8].

Less extensive investigation of dislocation structure has been carried out in deformed zinc single crystals. Of course also in this case a qualitative correlation between dislocation structure and the stages of the work hardening curve has been found [8]. It has been shown that the strain hardening in stage *A* in zinc single crystals is controlled by interaction of the basal-basal dislocations causing formation of dipoles and multipoles. The transition from stage *A* to stage *B* is characterized by the presence of the forest dislocations in non-basal slip systems [9]. In contrast to magnesium where the forest dislocations are tied with the primary ones, in the case of zinc they are formed in the pyramidal slip system $\{11\bar{2}2\}\ \langle 11\bar{2}3\rangle$. In both cases, however, formation of forest dislocations is associated with relaxation of the inner stress in the primary slip system.

So far less attention has been paid to the investigations of evolution of dislocation structure at very low temperatures [34, 35]. Using transmission electron microscopy Sharp et al. [34] have observed dislocation structure in magnesium deformed

by basal slip at 77 K. They have shown that the dislocation distribution at 77 K is more homogeneous than that at room temperature. In specimens deformed to 37,5% shear strain (at 77 K) the dislocation network is formed due to interaction between basal dislocations with different Burgers vectors. Forest dislocations are practically not present. Lavrentev et al. [35] have investigated the dislocation structure in magnesium samples deformed by simple shear in the basal slip at 77 K. On

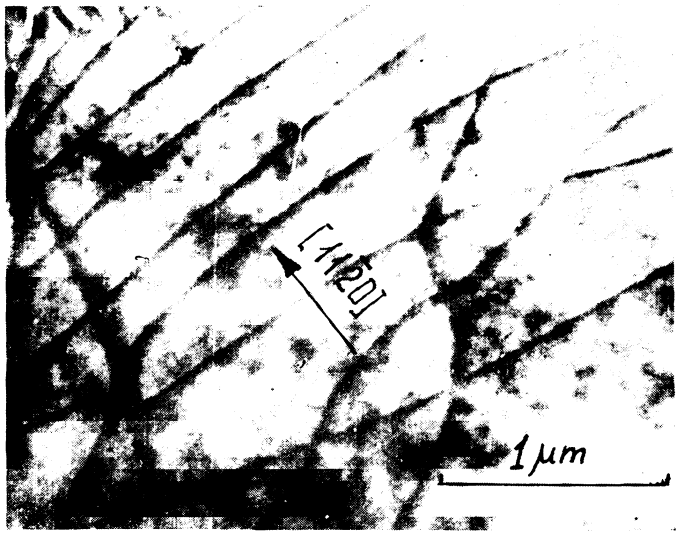

Fig. 14. Typical dislocation structure formed in magnesium single crystal deformed to 30% at 77 K [35].

the basis of both experimental studies [34, 35] one can conclude that the dislocation structure developed in stage A of the work hardening curve is characterized by isolated, almost straight-line basal dislocations close to the edge orientation, and rarely dipoles and multipoles. The latter two comprise basal dislocations of the edge type. The dislocation structure formed at 77 K differs from that at 300 K by the fact that at lower temperature the dislocations belonging to the secondary basal slip systems are not practically observed (Fig. 14).

In the transition from stage A to stage B ($a \approx 130\%$) the densities of primary and secondary basal dislocations are practically the same about $5 \cdot 10^8$ cm^{-2}. Dislocation grids of nonequilibrium shape (Fig. 15) as well as pile-up of the primary basal dislocations of the same sign (consisting of 10 to 15 dislocations) are observed at the end of stage A. The presence of the double cross slip of basal screw dislocations through the prismatic planes is typical for crystals deformed at 300 K. Due to this process the forest dislocations in prismatic slip system $\{1\bar{1}00\}\langle 11\bar{2}0\rangle$ are formed. On the other hand, cross slipping and the forest dislocations formation are not

observed in crystals deformed to the end of stage *A* at 77 K. At the same time the density of fine slip lines at such strains at 77 K is about 3–4 times higher than that at 300 K.

As to other metals with h.c.p. lattice there is practically lack of experimental results regarding the dislocation structure evolution. We believe that we can made

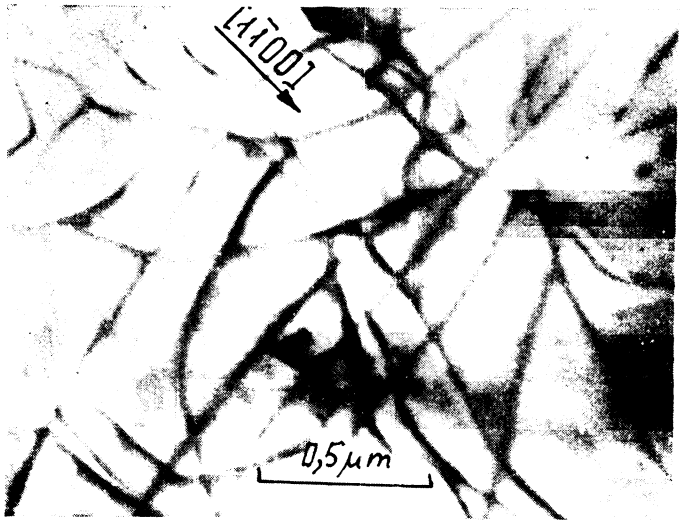

A)

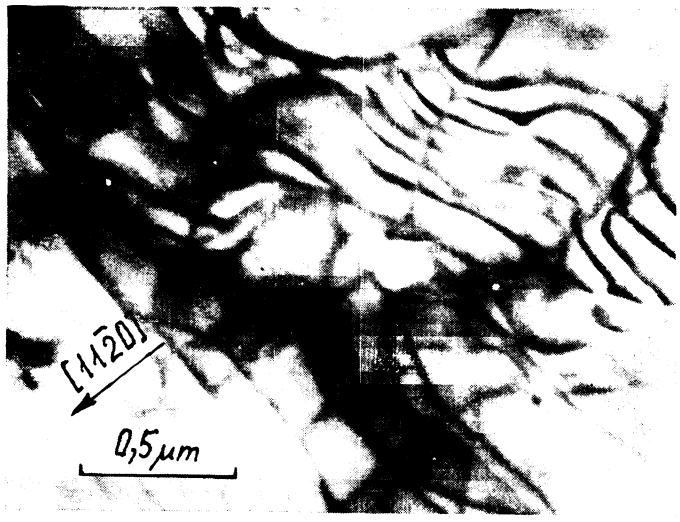

B)

Fig. 15. Dislocation structure formed in magnesium single crystal deformed to 130% at 77 K [35].

some conclusions concerning stages of the work hardening curve if we use experimental results on the dislocation structure of Zn single crystals deformed at 300 K, and Mg crystals deformed at 77 and 300 K.

Lavrentev [8] has shown that the transition from stage *A* to stage *B* at room temperature is characterized by formation of the forest dislocation in intersection slip planes and by an increase of the work hardening due to interaction between basal and prismatic planes (Mg single crystals) or basal and pyramidal dislocations (Zn single crystals). Motion of the basal dislocations is hindered by the forest dislocations ought to mutual recombination.

On the basis of experimental measurements of the work hardening parameters in zinc single crystals with a given initial density of the forest dislocations Lavrentev has pointed one that the forest dislocations contribute significally to the strain hardening in stage *A* of the work hardening curve.

As mentioned above the dislocation structure formed during the low temperature deformation exhibits some peculiarities [34, 35]. The transition from stage *A* to stage *B* at 300 K is probably different from that at 77 K. In stage *A* at 300 K the moving dislocations are retarded by the forest dislocations just formed whereas at 77 K the obstacles for the moving basal edge dislocations are multipoles, grids and dislocation sheets. Because the cross slip at lower temperatures is more difficult one may conclude that the transition from stage *A* to stage *B* at 77 K is connected with a strong interaction along nonbalanced multipole structure elements disposed in parallel basal planes if a high density of active strain regions (about $10^5\ \mathrm{cm}^{-1}$) is reached [35].

The transition from stage *B* to stage *C* connected with decreasing of the work hardening rate is studied rarely. Two mechanisms have been proved to be of importance in this connection: the climb of edge dislocations and the cross slip of screw dislocations [40, 41]. Lukáč and Švábová [42] measured the stress τ_C at the beginning of stage *C* of the work hardening curve in zinc single crystals as a function of the temperature and of the strain rate. They calculated, according to the theory of Seeger [41], the stacking fault energy γ, which is about $0{,}370\ \mathrm{J/m^2}$. However, no direct observations of the dislocation structure in stage *C* of the work hardening curve have been made and therefore it is very difficult to identify hardening mechanism(−s) in stage *C*.

3.2. Dislocation density dependence of the flow stress in h.c.p. metals

Work hardening is sensitive to a change of the dislocation density during deformation. In order to find the influence of microstructural characteristics on macroscopic parameters of the work hardening curve it is necessary to explain a relation between the dislocation density and the flow stress. As mentioned above, a number of transmission electron microscopy studies has been reported for magnesium single crystals [8, 32, 34, 35].

Dependence of the shear stress on the basal dislocation density ϱ_b in stage A and on the total density $(\varrho_b + \varrho_p)$, where ϱ_p is the prismatic dislocation density, in stage B are given in Fig. 16. It is obvious that the relation between the flow stress τ and the dislocation density can be described by an equations of the type

$$\tau = \tau_k + \alpha\mu b\sqrt{\varrho} \tag{1}$$

where τ_k is the stress at $\varrho = 0$, b is the Burgers vector and α is an interaction constant. The value of α depends on the type of the dislocation interaction. Thus, for example, for basal slip deformed magnesium single crystals [36, 43] $\alpha_b = 0.2$ at stage A and $\alpha_b = 0.1$ at stage B where are also present the prismatic dislocations. Dependence of the basal dislocation density on the shear strain can be divided to two parts with different slopes for the strain about 160%, which corresponds to the transition from stage A to stage B of the work hardening curve.

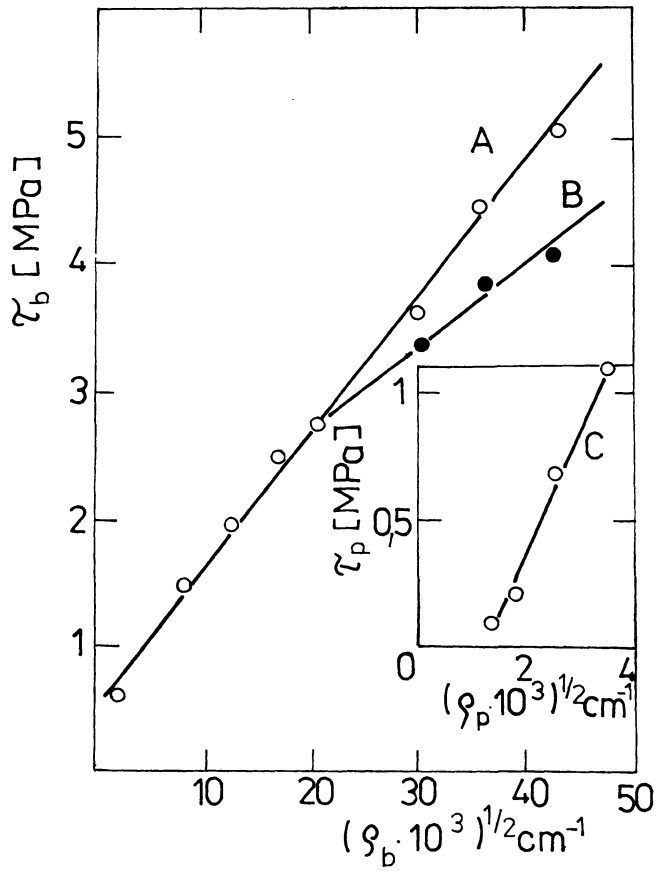

Fig. 16. Stress dependence of the density of basal dislocations ϱ_b at stage A and of basal and prismatic dislocations $\varrho_b + \varrho_p$ at stage B of the work hardening curve [8].

Lavrentev [8] has also investigated dependence of the dislocation density in the pyramidal slip system $\{11\bar{2}2\}\langle 11\bar{2}3\rangle$ on the shear stress for magnesium single crystals deformed by compression along [0001] direction. It was found that the $\tau - \varrho$ relation can be described by equation (1) with $\alpha = 0.9$ and $\tau_k = 4.5$ MPa. The value of α for the pyramidal slip system is higher than α for the basal-basal dislocation interaction. It is consistent with a hypothesis of Lavrentev [44] according to which α is essentially related to the energy gain due to a pairwise interaction of dislocations: the larger the energy gain the larger is α. Different types of dislocation interaction can give different contributions to the flow stress. Accordingly the $\tau - \varrho$ relation should be written not as eq. (1) but as the sum [8]

$$\tau = \tau_k + \sum \alpha_i \mu_i b_i \sqrt{\varrho_i} \tag{2}$$

where i indicates the dislocation interaction type. Thus, for example, for magnesium single crystals deformed by basal slip the eq. (2) has the following form:

$$\tau = \tau_k + \alpha_b \mu b \sqrt{(\varrho_b)} + \alpha_p \mu b \sqrt{\varrho_p} \tag{2a}$$

where $\alpha_b = 0.2$ at stage A and $\alpha_b = 0.1$ and $\alpha_p = 1$ at stage B; $\tau_k = 0.5$ MPa.

In contrary to $\alpha_b = 0.2$ obtained by Lavrentev [9], Hirsch and Lally [38] has found $\alpha_b = 0.05$. This discrepancy seems to arise from the different estimation of the dislocation density. Hirsch and Lally [38] have not taken into account a greater inhomogenity in the arrangement of dislocations in crystals.

Observations in magnesium single crystals deformed at 77 K [35] indicate that the dependence of the flow stress on the basal dislocation density may be also described by eq. (1) with $\alpha = 0.48$.

Therefore, we can assume that the equation (1) is universal describing the dislocation interactions of various types in h.c.p. metals investigated at 300 K and in Mg single crystals likewise at 77 K. It should be noted that more recently Lavrentev [45] presented an analysis of the available data regarding to the $\tau - \varrho$ relation for crystals of different lattice types (f.c.c., b.c.c., and h.c.p.). It was found that the $\tau - \varrho$ dependence should be written in the form of eq. (2).

The dislocation structure consisting of dipoles and multipoles is characteristic for stage A, as mentioned above. The $\tau - \varrho$ dependence given by eq. (1) observed in stage A is due to the fact that the interaction of intersection dislocations results in formation of dislocation network and of triple dislocation nodes. Because at the early stage in the deformation most of the retained dislocations have the primary Burgers vector [8, 32] there are not conditions for evolution the complex dislocation structure. Therefore the $\tau - \varrho$ dependence at the early stage of the deformation can be different from that given by eq. (1). It should be noted that the use of transmission electron microscopy to the onset of deformation is less effective since changes in the dislocation density are small. The dislocation density can be determined by etching. This method was used by Lavrentev et al. [46] for Mg single crystals deformed by basal slip at the early stage of the deformation. They deformed samples wih the orien-

tation which allowed deformation only in one of the three close packed directions in the basal plane at the shear strain rate of $2 \times 10^{-3}\ s^{-1}$. The investigated strain interval was 0–25%. The maximum strain (25%) was chosen so that etch-pits (about $6 \cdot 10^7\ cm^{-2}$) could be measured by means of optical microscope. One sample was deformed step-wise ($\Delta\tau \approx 0.1-0.2$ MPa). Fig. 17 shows the obtained dependence of the dislocation density on the flow stress (curve 1). It is evident that this dependence can be given in the form

$$\tau = \tau_k + \beta\varrho \tag{3}$$

where $\tau_k = 0.65$ MPa and $\beta = 1.25 \times 10^{-6}$ N if ϱ is measured in cm^{-2}.

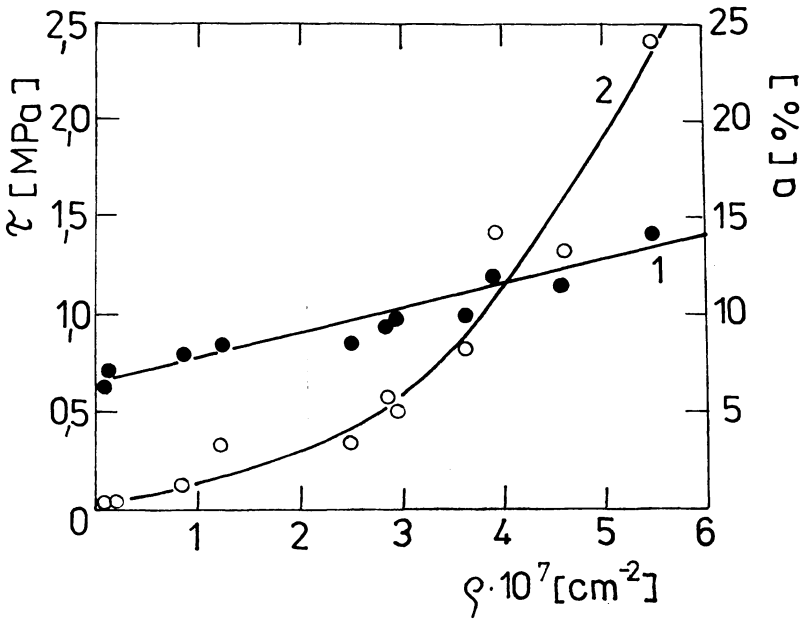

Fig. 17. Dependence of the flow stress on the basal dislocation density (curve 1) and variation of the basal dislocation density with shear strain (curve 2) for magnesium single crystals [46].

A theoretical analysis of the relation between the dislocation density and the flow stress in the case of the dipole structure gives [47]

$$\tau = \frac{\mu l}{2\pi}\left(\frac{1}{l} - \frac{1}{l+h}\right) \approx \frac{\mu l h}{2\pi l^2} \tag{4}$$

where h is the distance of the two dislocations perpendicular to the slip plane and l is the average distance of dipoles.

Investigations of the dislocation density dependence of the flow stress in zinc single crystals deformed in a wide temperature range from 1.5 to 300 K [48] have

demonstrated that the $\tau - \varrho$ dependence at the beginning of the deformation is of the form of eq. (1) with $\alpha = 0.24$. The value of α varies with temperature only as the temperature dependence of the shear modulus μ. The long-range flow stress component τ_μ estimated from this dependence is 0.24 MPa which is in good agreement with the value of the critical resolved shear stress $\tau_0 = 0.26$ MPa measured in the experiments.

The relation between the flow stress and the dislocation density is, in this case, determined only by the elastic long-range basal-basal dislocation interaction. It was observed that the dipole structure formed in the early stage of the deformation is unstable in zinc. The dipoles may disappear. This can be the cause of recovery processes observed in zinc crystals at room temperature [49].

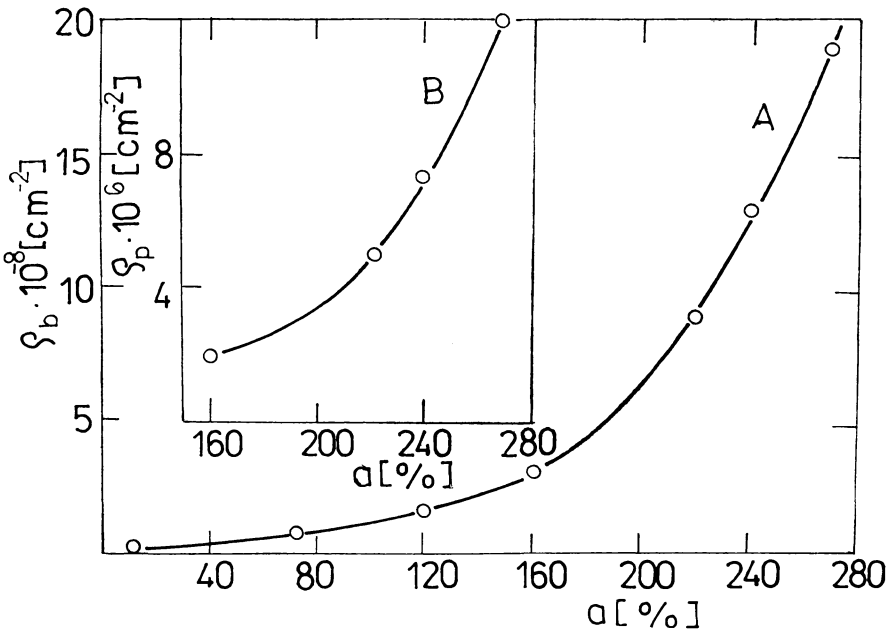

Fig. 18. Dependence of the basal dislocation density on the shear strain for magnesium single crystals at room temperature [8].

3.3. Dependence of the dislocation density on the shear strain in h.c.p. metals

The dependence of the dislocation density on the shear strain a for stage A and stage B in magnesium single crystals is given in Fig. 18 [8]. It is evident that the ϱ_b vs a dependence for a between 40 and 280% may be divided to two parts with different slopes. The change in the slope occurs at about 160% which corresponds to the transition from stage A to stage B of the work hardening curve. In Fig. 18 it is also shown the shear strain dependence of the prismatic dislocation density (curve II). The obtained dependences of the dislocation density on the flow stress τ and the shear

strain a enable one to construct the work hardening curve and to compare this constructed work hardening curve with that obtained directly. The same method has been used by Hirsch and Laly [32], too.

Experimental results [8] can be expressed as follows:

In stage A

$$\varrho_b^A = (0.5 \times 10^7 + 1.59 \times 10^8 a^{1.2})\,\mathrm{cm}^{-2}$$

and in stage B

$$\varrho_b^B = (4.5 \times 10^7 + 3.65 \times 10^7 a^4)\,\mathrm{cm}^{-2}$$

$$\varrho_p^B = (8.5 \times 10^5 + 2.42 \times 10^5 a^4)\,\mathrm{cm}^{-2}$$

The computed work hardening curve can be given in the forms:

In stage A

$$\tau_A = [50 + 137\,(a^{1.2} + 0.03)^{1/2}] \times 10^{-2}\ \mathrm{MPa}$$

and in stage B

$$\tau_B = [50 + 66\,a^2] \times 10^{-2}\ \mathrm{MPa}\,.$$

The calculated curve is in a quite reasonable agreement with the measured one.

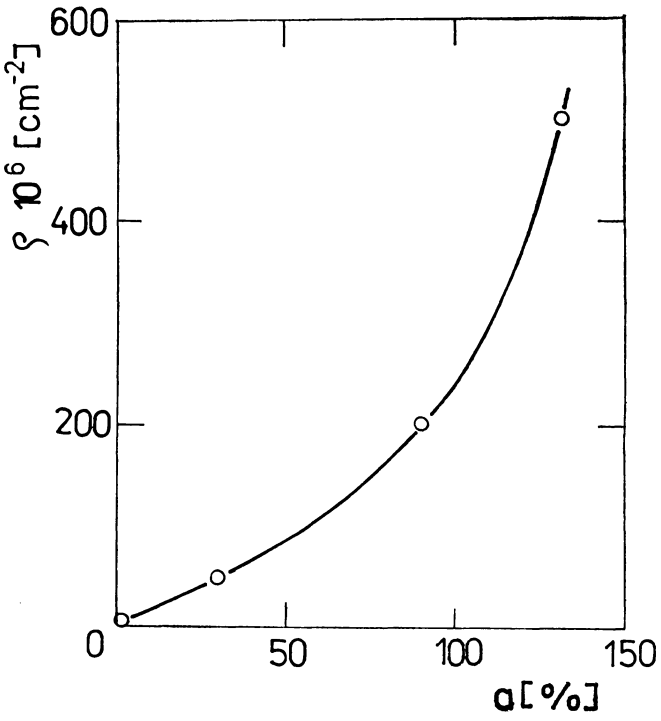

Fig. 19. Dependence of the basal dislocation density on the shear strain for magnesium single crystals at 77 K [35].

The $\varrho - a$ dependence at the beginning of the deformation ($a < 25\%$) in zinc single crystals [48] is plotted in Fig. 17 (curve 2). It is seen that the dependence is not linear. The change in the dislocation density with the shear strain $d\varrho/da$ decreases from an initial value of about $7.8 \times 10^8\ \mathrm{cm}^{-2}$ at the onset of the deformation to a final value of about 1.2×10^8 at higher strains. The value of $d\varrho/da$ at $a = 5\%$ is in agreement with electron microscopy observations in [9], where it has been shown that $d\varrho/da$ is the order of $10^8\ \mathrm{cm}^{-2}$.

The relation between the dislocation density ϱ and the shear strain a in stage A of magnesium single crystals deformed at 77 K [35] is found to be of the form

$$\varrho = \varrho_o + Aa^2 \tag{5}$$

where $\varrho_o = 1 \times 10^6\ \mathrm{cm}^{-2}$ and $A = 3.2 \times 10^8\ \mathrm{cm}^{-2}$. Fig. 19 shows a plot of this relation in the form ϱ versus a.

Combining the equations (1) and (5) one obtains an average stage A of the work hardening curve which is given by

$$\tau = \tau_o + \vartheta a \tag{6}$$

where ϑ is the work hardening rate.

Combining the equations (1), (5) and (6) one obtains the following relation for α [35]

$$\alpha = \vartheta/\mu b A^{1/2}\,. \tag{7}$$

It is seen that the value of the work hardening rate is directly connected with the value of the dislocation interaction coefficient α. Thus the increase of ϑ with decreasing temperature from 300 to 77 K as well as with it associated decrease in the length of stage A may be explained by a stronger dislocation interaction at 77 K which becomes evident quantitatively by an increase in α, dislocation and slip line densities at corresponding strains [35].

4. Some regularities of changes of the flow stress components

It is well-known that temperature may have a great influence on the CRSS and the other parameters of the work hardening curve of metal crystals. It is important to find a quantitative relation between the measured parameters and the dislocation structure and their changes with temperature.

4.1. Changes of the flow stress components with temperature

It is known that the flow stress can be separated to two components

$$\tau = \tau_s + \tau_\mu \tag{8}$$

where τ_s is a short-range component and τ_μ is a long-range component. It is interesting to find which of the components controlls the observed temperature dependence of

the CRSS (Fig. 3, 4). To solve this question Lavrentev et al. [4] have used two kinds of experiment. In the first kind the dislocation structure was created by deformation of samples to the stress $\tau(T_1)$ at temperature T_1 and then the samples were deformed to the CRSS at temperature T_2. It was found that the temperature dependence of the CRSS (Fig. 3) is independent of the previous deformation as can be seen from Table 2. This results may be explained supposing the long-range flow component τ_μ is constant in the temperature range from 1.5 to 300 K.

Table 2

The value of $\tau(T_1)\ \mu(300\text{ K})/\mu(T_1)$ and $\tau_0(T_2)\ \mu(300)/\mu(T_2)$

Experiment	T [K]	$\tau_0\mu(300\text{ K})/\mu(T)$ [MPa]
1	1.5	0.68
	4.2	0.29
2	1.5	0.72
	10	0.21
3	40	0.37
	10	0.24
4	40	0.41
	300	0.31

In the second kind of experiments Lavrentev et al. [4] estimated τ_s and τ_μ using the stress relaxation technique. The dislocation structure was also formed at various low tempetatures. The deformation and the stress relaxation followed at 300 K. Table 3 gives the values of the CRSS at various temperatures and the corresponding values of τ_μ (300 K) at 300 K. From these experimental results one can conclude that the temperature dependence of CRSS is controlled by the temperature dependence of τ_s

Table 3

The values of τ_0 and $\tau_\mu(300)$

T [K]	1.5	4.2	20	300
τ_0 [MPa]	0.73	0.32	0.30	0.25
$\tau_\mu(300\text{ K})$ [MPa]	0.27	0.25	0.28	0.22

This conclusion is also supported by measurements of the $\tau - \varrho$ dependence in zinc single crystals in the range 1.5–300 K [48]. The experiments revealed no temperature dependence of α in the second term of eq. (1). Thus, the second term in

eq. (1) contributes to the long-range component τ_μ. The temperature dependence of the CRSS could be due to the first term in eq. (1), i.e. τ_k and its short-range component.

We believe that τ_s controlls the temperature dependence of the CRSS not only in h.c.p. metals [50] but also in f.c.c. metals as stated in [1, 7, 12].

4.2. Deformation mechanisms at various temperatures

At low temperatures (below about 50 K) the yield-stress anomalies are observed for several f.c.c., b.c.c. and h.c.p. alloys [1, 10]. The explanation of the anomalies in the temperature dependence of the CRSS has atracted considerable attention in the literature. There are some proposed models to account for the low temperature dependence of the flow stress. The models take into account quantum tunnelling of dislocations through thermal barriers [51], significance of the attempt frequency [52], dynamic and inertial effects [53–55], and, of course, the thermally activated processes [1, 12, 50]. The models considering the dislocation line zero oscillations and quantum effects in the plasticity of crystals [52, 56] do not predict a sign change in $d\tau_0/dT$ in the temperature dependence of the CRSS. On the other hand, thermally activated dislocation mechanisms cannot be excluded in h.c.p. metals [57] and in some cases dislocation motion on the slip plane is controlled by a viscous damping mechanism [55, 58, 59].

It would be very interesting to decide whether the viscous drag or thermally activated motion of dislocation take place at low temperatures. One of methods which could give more information is the strain rate change experiment. The effect of strain changes on the flow stress is different for viscous drag and for thermally activated mechanisms. On the basis of strain rate change tests Lavrentev et al. [4] have concluded that the nonmonotonous temperature dependence of the CRSS for Zn single crystals (and probably for other h.c.p. metals) is due to occurrence of thermally activated processes. This conclusion seems to be valid not only for h.c.p. metals but also for other materials. To decide what processes are the rate-controlling mechanisms is, at present, impossible.

4.3. Effects of stress states on some parameters of the work hardening curve

An analysis of the dislocation structure during straining given in section 3 shows that the transition from stage A to stage B of the work hardening curve (in crystals deformed by basal slip) is due to forest dislocation formation in the intersecting planes. This result may help to explain the experimentally observed differences in some parameters of the work hardening curve (the work hardening rate ϑ_A and the length of stage A a_A) if crystals are deformed using various loading methods (compression, tension, simple shear) as discussed in section 2. The observed differences in ϑ_A as well as a_A may be caused the fact that the component of the external stress which adds in the intersecting (forest) slip systems is higher in the case of deformation

either by compression or tension than in the deformation by simple shear. Due to this fact the activity of the intersecting slip systems may start earlier and therefore the forest dislocations may be formed. This means that the length of stage *A* should be shorter and the work hardening rate higher.

In f.c.c. metals the work hardening rate in stage I is increasing and the length of stage I decreasing with increasing temperature [2, 31]. In contrary to h.c.p. metals where there is only one easy basal glide plane, f.c.c. metals have eleven intersecting slip systems which are equivalent to the primary system. The components of the external stress in the intersecting slip become equal to the critical resolved shear stress. With increasing temperature it is to be expected that dislocation reactions between primary and secondary dislocations are easier and they contribute to the work hardening as well as to the transition form stage I to stage II of the work hardening curve [2, 31].

In the case of h.c.p. metals the values of the CRSS for the intersecting slip systems are much higher than those for the basal system. Likewise the temperature dependences of the CRSS for various slip systems are different. Similar differences do not exist in f.c.c. metals.

5. Conclusions

Analysis of the recently obtained experimental results allows to explain a number of new regularities of the temperature dependence of the work hardening parameters.

It is concluded that the nonmonotonous temperature dependence of the CRSS is caused by the variation of the short-range flow stress component. It is shown that thermally activated deformation mechanisms take place in the whole temperature range from 1.5 to 300 K. The occurrence of the yield-stress anomalies is influenced by the solute atoms, even if the character of the solute atoms effect is not unambiguous. The anomaly is more pronounced with increasing concentration of solute in Zn [4], Cd [6] and Cu [19] while it is amaller in Be alloyed with Cu [26].

The character of the temperature dependence of the CRSS is also influenced by the dislocation structure. As indirect evidence may serve experiments on cadmium – based alloys single crystals deformed with different loading methods at very low temperatures. Different kinds of the observed temperature dependences of the CRSS may be caused by different methods for determining the CRSS [5, 6, 21, 60]. In order to explain the effect of the dislocation structure on the temperature dependence of the CRSS further experimental investigations are necessary.

In a number of the works concerning the nonmonotonous temperature dependence of the CRSS attempts have been made to find the form and height of obstacles and to identify the rate-controlling mechanism. It is obvious that there is no single process and therefore it is impossible to ascribe the estimated activation parameters to one process.

The work hardening behaviour seems to be a result of different processes. Contributions of the processes may be different within different temperature ranges. In order to estimate the contributions further experimental and theoretical works are needed.

References

[1] PUSTOVALOV, V. V.: DrSc Thesis. FTINT, Academy of Sciences of USSR, Kharkov 1973.
[2] SEEGER, A.: Handbuch der Physik VII/2. Springer, Berlin 1958.
[3] LAVRENTEV, F. F., SALITA, O. P., SHUTYAEV, P. D.: Fiz. Met. Metalloved,. 43 1977, 1300.
[4] LAVRENTEV, F. F., SALITA, O. P., SHUTYAEV, P. D.: Fiz. Met. Metalloved., 41 1976, 412.
[5] STULÍKOVÁ, I., LUKÁČ, P., SHKLAREVSKAYA, G. I.: Phys. Status Solidi, (a) 41 1977, K197.
[6] WIELKE, B., CHALUPKA, A., KAUFMANN, B. LUKÁČ, P., SVOBODOVÁ, A.: Z. Metallkde 70 1949, 85.
[7] PUSTOVALOV, V. V., in: Fizika deformatsionnogo uprochnenya monokristallov. Naukova Dumka, Kiyev 1972, p. 128.
[8] LAVRENTEV, F. F., DrSc.: Thesis. FTINT, Academy of Sciences of USSR, Kharkov 1973.
[9] LAVRENTEV, F. F., in: Fizika deformatsionnogo uprochnenya monokristallov, Naukova Dumka, Kiyev 1972, 107.
[10] STARTSEV, V. I., ILICHEV, V. YA., PUSTOVALOV, V. V.: Plastichnost i prochnost metallov i splavov pri nizkich temperaturach. Metallurgiya, Moskow 1975.
[11] WIELKE, B., TIKVIC, W. SVOBODOVÁ, A., LUKÁČ, P.: Acta Met. 25 1977, 1071.
[12] LANDAU, A. I., PARKHOMENKO, A. T., PUSTOVALOV, V. V.: Fizika nizkich temperatur 1 1975, 193.
[13] LAVRENTEV, F. F., POKHIL, YU. A.: Fiz. Met. Metalloved. 34 1972, 1270.
[14] POKHIL, YU. A.: Kristall u. Technik 9 1974, 1179.
[15] LAVRENTEV, F. F., SOKOLSKIJ, S. V.: Fiz. Met. Metalloved. 41 1976, 857.
[16] VLADIMIROVA, V. L., in: Fizicheskiye processy plasticheskoy deformatsii pri nizkich temperaturach. Nakova Dumka, Kiyev 1974, p. 68.
[17] VLADIMIROVA, V. L., LAVRENTEV, F. F., POKHIL, YU. A., in: Fizicheskiye processy plasticheskoy deformatsii pri nizkich temperaturach. Naukova Dumka, Kiyev 1974, p. 44.
[18] SCHMID, E., BOAS, W.: Kristallplastizität. Springer, Berlin 1935.
[19] SUZUKI, T., in: Dislocation Dynamics. Mc Graw-Hill, New York 1968, p. 551.
[20] SOLDATOV, V. P., OSETSKII, A. I., STARTSEV, V. I., NATSIK, V. D.: Fiz. Met. Metalloved. 39 1975, 669.
[21] NAVRÁTIL, V., LUKÁČ, P., SOLDATOV, V. P.: Phys. Statu. Solidi, (a) 54 1979, K 175.
[22] STOHR, J. F., POIRIER, J. P.: Phil. Mag. 25 1972, 1313.
[23] ESCARAVAGE, C., BACH, P., CHAMPIER, C., in: Proc. ICSMA 2, vol. 1. ASM, Asilomar 1970, p. 299.
[24] URAKAMI, A., MESHII, M., FINE, M. E., in: Proc. ICSMA 2, vol. 1. ASM, Asilomar 1970, p. 272.
[25] FLYNN, P. W., MOTE, J., DORN, J. E.: Trans. AIME 221 1961 1148.
[26] PAPIROV, I. I., TICHINSKII, G. F., KRISTENKO, I. N., AVOTIN, S. S., KAPCHERIN, A. S.: Priroda plasticheskoy deformatsii Be. Naukova Dumka, Kiyev 1977.
[27] WIELKE, B.: Phys. Status Solidi (a) 33 1976, 241.
[28] WIELKE, B., CHALUPKA, A., SCHOECK, G., in: Strength of Metals and Alloys, vol. 1. Pergamon Press, Toronto 1979, p. 65.

[29] HONEYCOMBE, R. W. K.: The Plastic Deformation of Metals. E. Arnold Ltd., London 1968.
[30] LUKÁČ, P., TROJANOVÁ, Z., SVOBODOVÁ, A.: Czech. J. Phys. B 31 1981, 133.
[31] BERNER, R., KRONMÜLLER, H., in: Moderne Probleme der Metallphysik. Springer, Berlin 1965, p. 167.
[32] HIRSCH, P. B., LALLY, J. S.: Phil. Mag. 12 1965, 595.
[33] SHARP, J. V., CHRISTIAN, J. W.: Phys. Status Solidi 11 1965, 831.
[34] SHARP, J. V., MAKIN, M. J., CHRISTIAN, J. W.: Phys. Status Solidi 11 1965, 845.
[35] LAVRENTEV, F. F., POKHIL, Yu. A., SOKOLOVSKY, S. V., in: Strength of Metals and Alloys, vol. 1. Pergamon Press, Toronto 1979, p. 163.
[36] LAVRENTEV, F. F., POKHIL, YU. A.: Mater. Sci. Eng. 18 1975, 261.
[37] LAVRENTEV, F. F., POKHIL, YU. A.: Phys. Status Solidi (a) 32 1975, 227.
[38] CHEN, H. S., GILMAN, J. J., HEAD, A. K.: J. Appl. Phys. 35 1964, 2502.
[39] KRATOCHVÍL, P.: Phil. Mag. 13 1966, 267.
[40] BASINSKI, Z. S.: Austr. J. Phys. 12 1960, 284.
[41] SEEGER, A., in: Rep. Conf. Defects in Solids Phys. Soc., London 1955, p. 340.
[42] LUKÁČ, P., ŠVÁBOVÁ, M.: Phys. Status Solidi 8 1965, 187.
[43] LAVRENTEV, F. F., POKHIL, YU. A.: Izvestiya Academy of Sciences of USSR 38 1974, 1540.
[44] LAVRENTEV, F. F., in: Fizika deformatsionnogo uprochnenya monokristallov. Naukova Dumka, Kijev 1972, p. 107.
[45] LAVRENTEV, F. F.: Mater. Sci. Eng. 46 1980, 191.
[46] LAVRENTEV, F. F., SALITA, O. P., SOKOLSKIJ, S. V., in: Rep. Conf. Deformation Hardening of Steel and Alloys, Barnaul 1979, p. 47.
[47] FRIEDEL, J.: Dislocations. Pergamon Press, Oxford 1964.
[48] LAVRENTEV, F. F., SALITA, O. P., SHUTYAEV, P. D.: Fiz. Met. Metalloved. 48 1979, 1026.
[49] PRICE, P. B., in: Electron Microscopy and Strength of Crystals. Interscience, New York 1963, p. 41.
[50] LUKÁČ, P., TROJANOVÁ, Z., in: Strength of Metals and Alloys, vol. 2. Pergamon Press, Toronto 1979, p. 1061.
[51] MOTT, N. F.: Phil. Mag. 1 1956, 568.
[52] NATSIK, V. D., OSETSKII, A. I., SOLDATOV, V. P., STARTSEV, V. I.: Phys. Status Solidi (b) 54 1972, 99.
[53] SUZUKI, T., ISHII, T., in: Physics of Strength and Plasticity. MIT Press, Cambridge 1969, p. 159.
[54] GRANATO, A. V.: Phys. Rev. B 4 1971, 2196.
[55] VREELAND, T., JR., JASSBY, K. M.: Mater. Sci. Eng. 7 1971, 95.
[56] FELTHAM, P.: Phys. Status Solidi (b) 98 1980, 301.
[57] LUKÁČ, P.: J. Sci. Ind. Res. 32 1973, 569.
[58] POPE, D. P., VREELAND, T., JR., WOOD, D. S.: J. Appl. Phys. 38, 1967, 4011.
[59] SCHWARZ, R. B., LABUSCH, R.: J. Appl. Phys. 49 1978, 5174.
[60] LUKÁČ, P., STULÍKOVÁ, I., NAVRÁTIL, V.: Czech. J. Phys. B 31 1971, 130.